

Optimal threshold in CT quantification of emphysema

Zhimin Wang · Suicheng Gu · Joseph K. Leader ·
Shinjini Kundu · John R. Tedrow · Frank C. Scirba ·
David Gur · Jill M. Siegfried · Jiantao Pu

Received: 4 July 2012 / Revised: 24 August 2012 / Accepted: 30 August 2012 / Published online: 1 November 2012
© European Society of Radiology 2012

Abstract

Objectives To determine the optimal threshold by quantitatively assessing the extent of emphysema at the level of the entire lung and at the level of individual lobes using a large, diverse dataset of computed tomography (CT) examinations. **Methods** This study comprises 573 chest CT examinations acquired from subjects with different levels of airway obstruction (222 none, 83 mild, 141 moderate, 63 severe and 64 very severe). The extent of emphysema was quantified using the percentage of the low attenuation area (LAA%) divided by the total lung or lobe volume(s). The correlations between the extent of emphysema, and pulmonary functions and the five-category classification were assessed using Pearson and Spearman's correlation coefficients, respectively. When quantifying emphysema using a density mask, a wide range of thresholds from -850 to -1,000 HU were used.

Results The highest correlations of LAA% with the five-category classification and PFT measures ranged from -925 to -965 HU for each individual lobe and the entire lung. However, the differences between the highest correlations and those obtained at -950 HU are relatively small.

Conclusion Although there are variations in the optimal cut-off thresholds for individual lobes, the single threshold of -950 HU is still an acceptable threshold for density-based emphysema quantification.

Key Points

- CT is widely used to assess the severity of emphysema
- Density mask technique helps clinicians assess the extent of emphysema with CT
- A standardised cut-off for density mask analysis at lobe level is desirable
- -950 HU is acceptable for density-based emphysema quantification at the lobar level

Z. Wang · S. Gu · J. K. Leader · D. Gur · J. Pu (✉)
Department of Radiology, University of Pittsburgh,
Pittsburgh, PA 15213, USA
e-mail: puj@upmc.edu

S. Kundu
School of Medicine, University of Pittsburgh,
Pittsburgh, PA 15213, USA

J. R. Tedrow
Department of Internal Medicine, University of Pittsburgh,
Pittsburgh, PA 15213, USA

F. C. Scirba
Division of Pulmonary and Critical Care Medicine,
University of Pittsburgh,
Pittsburgh, PA 15213, USA

J. M. Siegfried
Department of Pharmacology & Chemical Biology,
University of Pittsburgh,
Pittsburgh, PA 15232, USA

Keywords Chronic obstructive pulmonary disease · Computed tomography · Pulmonary emphysema · Density mask · Lobe segmentation

Introduction

The density of areas of emphysema depicted on computed tomography (CT) typically ranges from -900 to -1,024 Hounsfield Units (HU) [1]. Hence, a straightforward way of quantitatively assessing the extent of emphysema is to compute the low attenuation areas (LAA) under a specific threshold. Originally, Müller et al. [2] suggested a threshold of -910 HU for this density mask analysis. Later, Gevenois et al. [3] explained that a threshold of -950 HU correlated more closely with the macroscopic pathological features of emphysema. Since then, a threshold of -950 HU has been commonly used for density-based emphysema quantification [4–7].

However, recently, Madani et al. [8] suggested that a cut-off of -960 HU or -970 HU might yield more accurate assessment of the extent of emphysema. Therefore, there is no consensus on the optimal threshold for density-based emphysema quantification.

Often, a global index is computed to quantify the severity of emphysema by measuring the ratio of the low attenuation area below a specific threshold as a fraction of the entire lung volume [9]. As a global measure, this index ignores the fact that the density of emphysema may vary regionally throughout the lung. Considering that pulmonary lobes are relatively independent functional units with their own vascular and airway branches, there has been increasing interest in investigating the lobar distribution of emphysema [10–14]. Given the heterogeneity of emphysema, it remains an open question whether different thresholds are needed to accurately quantify emphysema in individual lobes. Different thresholds have been employed by investigators to quantify the extent of emphysema at the individual lobe level. For example, when the threshold was set at -910 HU, Saitoh et al. [10] found that the distribution of emphysema was different in the upper and lower lobes; when the threshold was set at -950 HU, Mohamed Hoesein et al. [14] found that subjects with upper lobe predominant emphysema tended to have a more rapid decline in measures of pulmonary function than those with lower lobe predominant emphysema; when investigating the relationship between pulmonary function and normal lobar volume, Matsuo et al. [13] also used -950 HU as the cut-off threshold. Given the heterogeneity of emphysema, it may be desirable to have a standardised cut-off threshold for density mask analysis in clinical practice.

In this study, we systematically investigated how LAA% varies with different thresholds on quantitative CT analysis of pulmonary emphysema at levels of both the individual lobe and the entire lung. A large and diverse dataset consisting of 573 chest CT examinations was collected from a chronic obstructive pulmonary disease (COPD) study. Here, our objective was to determine whether an optimal threshold can be used for more accurate and consistent quantification of emphysema for each pulmonary lobe. At the same time, we also assessed how CT densitometric measurements among these lobes correlate with the COPD severity and the commonly used pulmonary function test (PFT) measurements (e.g. forced expiratory volume in 1 s [FEV_1]).

Materials and methods

Study population

The study population consisted of 573 consenting subjects participating in an NIH-sponsored Specialized Centre for Clinically Oriented Research (SCCOR) in COPD at the

University of Pittsburgh. SCCOR subjects were primarily recruited from the Pittsburgh Lung Screening Study cohort. It is a tobacco-exposed cohort and includes a spectrum of obstructive lung disease severity. Inclusion criteria for enrolment required an age >40 years and at least a 10-pack-year history of tobacco use. The subjects underwent pre- and post-bronchodilator spirometry and plethysmography tests, measurements of lung diffusion capacity, impulse oscillometry, demographic and medical history questionnaires and a chest CT examination. All subjects were smokers with an average smoking history of 58.3 pack-years. These individuals were classified using a five-category classification, namely: (1) no airflow obstruction (None), (2) mild obstruction (GOLD I), (3) moderate obstruction (GOLD II), (4) severe obstruction (GOLD III) and (5) very severe obstruction (GOLD IV). Subjects that have $FEV_1/FVC < 70\%$ were classified into GOLD stages I–IV according to the Global Initiative for Obstructive Lung Disease (GOLD) [15]. The subjects that do not meet the GOLD classification were classified as “None”. All procedures were performed under a University of Pittsburgh Institutional Review Board-approved protocol (no. 0612016) and written informed consent was obtained for each subject. The involved SCCOR subject demographics are summarised in Table 1.

Acquisition of thin-section CT examinations

The CT examinations were performed using 64-detector CT (LightSpeed VCT; GE Healthcare, Waukesha, WI, USA) with subjects holding their breath at end-inspiration. The

Table 1 Subject demographics ($n=573$)

Parameter	Mean (\pm SD) or count (%)
Sex male	310 (54.1 %)
Age	63.9 (± 5.4)
Pack years	58.3 (± 33.0)
Height(cm)	169.4 (± 9.4)
Weight(kg)	80.0 (± 15.95)
RV % predicted	127.6 (± 53.2)
RV/TLC %	44.2 (± 12.7)
FEV_1 (litre)	2.15 (± 0.94)
FEV_1 % predicted	74.8 (± 28.5)
FEV_1/FVC %	60.8 (± 17.7)
DL_{CO} % predicted	66.4 (± 22.9)
Five-category classification	
NONE	222 (38.7 %)
GOLD I	83 (14.5 %)
GOLD II	141 (24.6 %)
GOLD III	63 (11.0 %)
GOLD IV	64 (11.2 %)

TLC total lung capacity, *RV* residual volume, *FVC* functional vital capacity, *FEV₁* forced expiratory volume in 1 s, *DL_{CO}* diffusing lung capacity of carbon monoxide

CT datasets were acquired using a helical technique without contrast medium at the following parameters: 32×0.625 mm detector configuration, 0.969 pitch, 120-kVp tube energy, 250-mA tube current, and 0.4-s gantry rotation (or 100 mAs). Images were reconstructed to encompass the entire lung field in a 512×512 -pixel matrix using the GE “bone” kernel at 0.625-mm section thickness and 0.625-mm interval. The “bone” kernel was used because of its ability to analyse both the parenchyma and airways [16].

Quantification of the extent of emphysema

Computerised schemes were used to process the CT examinations objectively and efficiently. The extent of emphysema at the levels of both the entire lung and individual lobes was quantified. First, a three-dimensional (3D) adaptive border marching algorithm described by Pu et al. [17] was used to identify the entire lung volume. Second, pulmonary fissures were detected using a computational geometry approach [18]. Third, individual lobes were identified by representing the pulmonary fissures as implicit surface functions [19]. Detailed descriptions of these computerised schemes have been reported elsewhere [17–19]. The final segmentation results were carefully inspected and verified by three independent image analysts. If the computerised schemes failed to accurately identify individual lobes, we manually delineated or refined the pulmonary fissure before applying the automated lobe segmentation scheme. Several examples in Fig. 1 are used to demonstrate the performance of the identified lobe segmentation scheme in the presence of severe emphysema.

In this study, the percentage of the LAA divided by lung or lobe volume(s) was used as an index of the extent of emphysema [20–23]. A wide range of thresholds, ranging

from -850 HU to $-1,000$ HU in intervals of 5 HU, were tested. The upper bound of -850 HU was selected because of the weak correlation between emphysema severity and LAA% at the threshold of -856 HU [24]. The lower boundary of $-1,000$ HU was chosen because the radiodensity of air is typically defined as $-1,000$ HU [25]. LAA% was computed at the levels of the entire lung, individual lobes (RUL, right upper lobe; RML, right middle lobe; RLL, right lower lobe; LUL, left upper lobe; LLL, left lower lobe), the upper lobe (RUL + RML + LUL), the lower lobe (RLL + LLL), the left lung and the right lung.

Statistical data analysis

All statistical analyses were performed using Excel (Microsoft, Redmond, WA, USA) and SAS (SAS Institute, Cary, NC, USA). We computed the mean volumes and the LAA% for each individual lobe and the entire lung. These results are expressed as mean \pm standard deviation (SD). Pearson correlation coefficients were used to assess the correlation between LAA% under different thresholds in individual lobes or the whole lung and PFT measures. In particular, we investigated whether the correlation would be different when the non-COPD subjects were included or excluded. When assessing the correlation between the five-category classification and LAA% under different cut-off thresholds, Spearman analysis was used. In addition, the correlations between lobe volume and emphysema severity based on our five-category classification were assessed. A *P* value less than 0.001 was considered statistically significant. The post-bronchodilator PFT measurements used in the correlation analyses included: (1) the residual volume (RV)/total lung capacity (TLC) ratio, (2) RV % predicted, (3) forced expiratory volume in 1 s (FEV_1), (4) FEV_1 % predicted, (5)

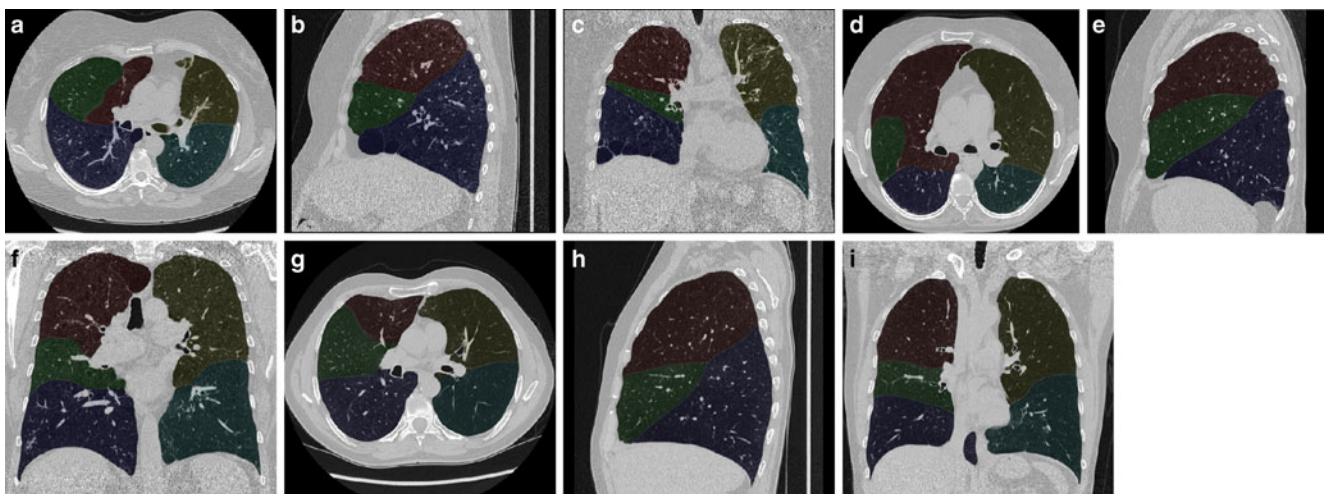


Fig. 1 Examples demonstrating the performance of the computerised schemes [16–18] in lobe identification in the presence of severe emphysema (GOLD = 4 for all three examples). (a)–(c) Example 1; (d)–(f) Example 2; and (g)–(i) Example 3

FEV₁/functional vital capacity (FVC) ratio and (6) diffusing lung capacity of carbon monoxide (DLco %) predicted.

Results

After the application of the lobe segmentation scheme to the collected 573 CT examinations (Table 1), the volumes of each individual lobe, the upper lobe, the lower lobe, the left lung, the right lung and the entire lung along their means (\pm SD) is summarised in Table 2. In Table 2, the LAA and LAA% obtained at the threshold of -950 HU were also listed. The LAA% ranged from 12.3 % to 18.4 %. In LAA%, there was no obvious difference between the left lung and the right lung, but there were differences between the upper lobe and the lower lobe. The average LAA% for each individual lobe under different thresholds is shown in Fig. 2, and the average LAA% for the upper lobe, the lower lobe, the right lung, the left lung and the entire lung under different thresholds is shown in Fig. 3.

The Spearman correlations between LAA% under different thresholds for individual lobes and the five-category classification are shown in Fig. 4, demonstrating a strong association between LAA% and the five-category classification regardless of the threshold. It can be seen that the thresholds corresponding to the highest correlation vary for each lobe. For example, for RUL, the optimal threshold is -935 HU ($r=0.649$, $P<0.001$); for RML, the optimal threshold is -945 HU ($r=0.521$, $P<0.001$). The computed results at different thresholds of the above correlations at the level of the upper lobe, the lower lobe, the left lung, the right lung and the entire lung are shown in Fig. 5, demonstrating a strong association for all thresholds ($r>0.631$, all P

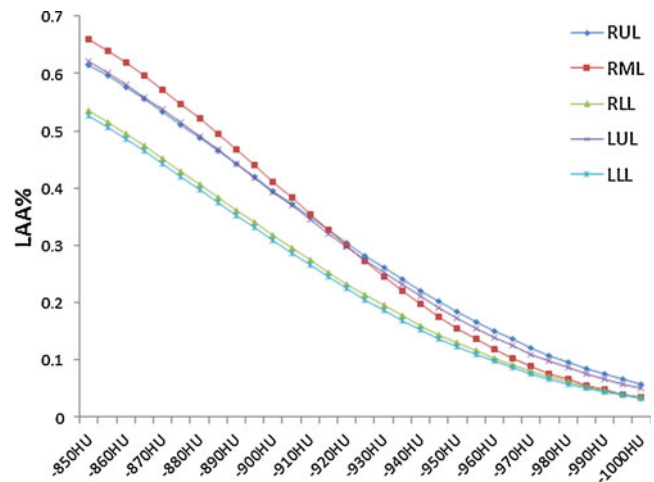


Fig. 2 Average LAA% for each individual lobe under different thresholds

values <0.001). It can be seen that the LAA% of the upper lobe and the right lung have a slightly higher association with the five-category classification than the LAA% of the lower lobe and the left lung at the same thresholds. The differences between the highest correlation coefficients and those at -950 HU were summarised in Table 3.

The computed Pearson correlation coefficients between the LAA% and the PFT measurements are listed in Table 4. The LAA% showed strong correlations with airflow obstruction measurements, such as FEV₁% predicted ($r=0.578$ – 0.726 , $P<0.001$), FEV₁/FVC ratio ($r=0.634$ – 0.795 , $P<0.001$) and DLco% predicted ($r=0.528$ – 0.707 , $P<0.001$). For lung capacity-related measures, such as RT/TLC ratio and RV% predicted, the LAA% only showed moderate associations. Conversely, the

Table 2 Volume, low attenuation area (LAA), and the percentage of LAA (LAA%) for each individual lobe, the upper lobe, the lower lobe, the left lung, the right lung and the entire lung

	Volume	LAA ^a	LAA% ^b
RUL	1.17 \pm 0.36	0.24 \pm 0.22	18.4 \pm 12.2
RML	0.51 \pm 0.18	0.08 \pm 0.06	15.5 \pm 8.7
RLL	1.28 \pm 0.36	0.18 \pm 0.16	13.0 \pm 9.5
LUL	1.37 \pm 0.37	0.25 \pm 0.19	17.3 \pm 10.3
LLL	1.20 \pm 0.37	0.16 \pm 0.15	12.3 \pm 9.3
Upper lobe	3.04 \pm 0.79	0.57 \pm 0.44	17.6 \pm 10.6
Lower lobe	2.48 \pm 0.69	0.34 \pm 0.30	12.8 \pm 9.2
Left lung	2.57 \pm 0.65	0.41 \pm 0.32	15.2 \pm 9.4
Right lung	2.95 \pm 0.68	0.49 \pm 0.38	15.9 \pm 10.1
Entire lung	5.52 \pm 1.30	0.91 \pm 0.68	15.6 \pm 9.7

All numerical values denote mean \pm SD in litres

^a LAA was calculated at -950 HU

^b LAA% (index of emphysema) was calculated at -950 HU

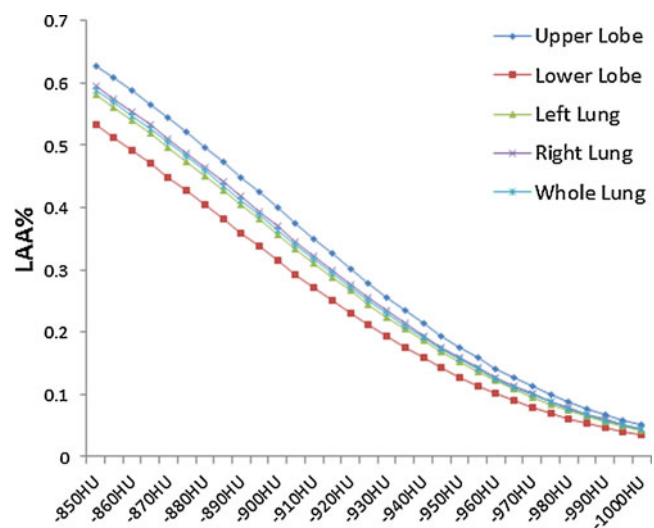
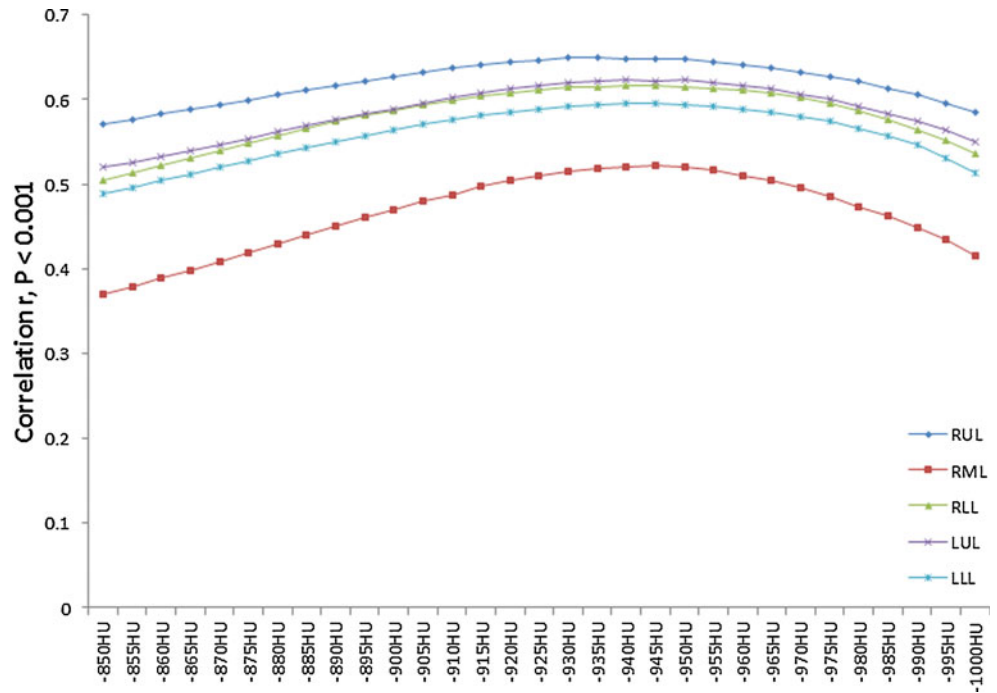


Fig. 3 Average LAA% for the upper lobe, the lower lobe, the left lung, the right lung and the entire lung under different thresholds

Fig. 4 Correlations between the LAA% and the five-category classification under different thresholds for each individual lobe. Highest correlation coefficient r and the corresponding threshold: (1) RUL, $r=0.649$ (–935 HU); (2) RML, $r=0.521$ (–945 HU); (3) RLL, $r=0.617$ (–940 HU); (4) LUL, $r=0.623$ (–940 HU); (5) LLL, $r=0.596$ (–945 HU). $P<0.001$ for all r values



LAA% of RML showed comparatively weak correlations with the PFT measures compared with the other lobes. It can be seen that the highest correlation coefficients and their corresponding cut-off thresholds were similar, no matter whether the non-COPD subjects were excluded or not.

Similar to the first correlation analysis between the LAA% and the five-category classification, the thresholds corresponding to the highest correlation coefficients ranged from –925 HU to –965 HU, and the differences between the highest correlation coefficients and those computed at the threshold of –950 HU are summarised in Table 5. In

addition, the significances (P values) of the differences between the highest correlation coefficients and those computed at –950 HU were also provided in Tables 3 and 5. Lastly, the correlations between lobe volumes and emphysema severity indexed in terms of five-category classification are shown in Fig. 6.

Discussion

The density mask method has been commonly used to assess the severity of COPD. Here, we systematically

Fig. 5 Correlations between the LAA% and the five-category classification under different thresholds for the upper lobe, the lower lobe, the left lung, the right lung and the entire lung. The highest correlation coefficient r and the corresponding threshold: (1) the upper lobe, $r=0.649$ (–940 HU); (2) the lower lobe, $r=0.631$ (–940 HU); (3) the left lung, $r=0.657$ (–945 HU); (4) the right lung, $r=0.677$ (–940 HU) and the entire lung, $r=0.676$ (–940 HU). $P<0.001$ for all r values

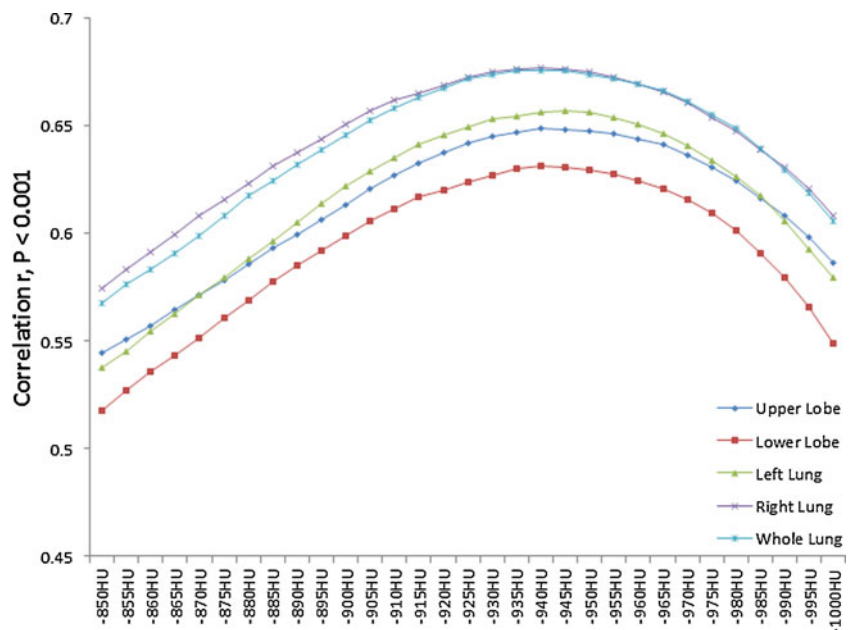


Table 3 Comparison of the highest correlation coefficients and those at -950 HU

	Correlation r between LAA% and five-category classification		
	Highest	-950 HU	Differences (% , significance)
RUL	0.649, -935 HU	0.647	0.002 (0.3 %, $P=0.476$)
RML	0.521, -945 HU	0.520	0.001 (0.2 %, $P=0.492$)
RLL	0.617, -940 HU	0.615	0.002 (0.3 %, $P=0.480$)
LUL	0.623, -940 HU	0.622	0.001 (0.2 %, $P=0.488$)
LLL	0.596, -940 HU	0.594	0.002 (0.3 %, $P=0.480$)
Upper lobes	0.649, -940 HU	0.648	0.001 (0.2 %, $P=0.488$)
Lower lobes	0.631, -940 HU	0.629	0.002 (0.3 %, $P=0.476$)
Left lung	0.657, -945 HU	0.656	0.001 (0.2 %, $P=0.488$)
Right lung	0.677, -940 HU	0.675	0.002 (0.3 %, $P=0.476$)
Whole Lung	0.676, -940 HU	0.674	0.002 (0.3 %, $P=0.476$)

All P value < 0.001

investigated the impact of threshold selection on the accuracy of assessing the extent of emphysema. This study has a number of unique merits. First, a relatively large, diverse dataset was used. To the best of our knowledge, few investigations have used a dataset as large as ours. A large dataset enables a robust investigation of the underlying relationship between density mask and emphysema extent. Second, the correlations between emphysema extent at different thresholds and pulmonary functions are studies not only at the level of the entire lung but also at the level of individual lobes. This regional analysis may verify whether a uniform threshold is sufficient to quantitatively assess the extent of emphysema. As a result, the ultimately determined optimal threshold may facilitate a more accurate assessment of emphysema extent. Third, our study verified that using a single cut-off threshold for emphysema assessment could achieve a reasonable accuracy. Finally, compared with previous investigations, this study considers a larger number of PFT measures.

In this study, not only the LAA% of each individual lobe but also the LAA% of the entire lung were computed. We found that the five-category classification was strongly correlated with LAA% under thresholds ranging from -850 to -1,000 HU. There were slight variations in the optimal thresholds corresponding to the highest correlation coefficients and those obtained at -950 HU do not vary significantly, and the percentage difference ranges from 0.2 % to 0.3 % (Table 3). This may suggest that the threshold of -950 HU is appropriate for emphysema quantification at the level of individual lobes. We arrive at the same threshold of -950 HU when similar analysis is repeated between the LAA% and pulmonary function (the percentage difference ranges from 0 % to 2.0 %). In fact, our results verified the conclusion reported in Pescarolo et al. [26], where the authors explained that there was significant correlation ($r=-0.7$, $P<0.001$) between the five-category

classification and the extent of emphysema. However, in the study of Pescarolo et al. [26], only 43 CT examinations were used.

When studying the correlation between emphysema extent and pulmonary function, Saitoh et al. [10] showed a strong correlation in the upper lobes, and Matsuo et al. [13] found that the LAA% of RLL and LLL had stronger correlations with VC, FEV₁ and DLco. However, in our study with a relatively large dataset, we failed to observe obvious difference in correlation coefficients between the upper lobes and the lower lobes, although the correlation coefficients for the upper lobes were also higher than those for the lower lobes. The small sample sizes (i.e. $n=50$ of Saitoh et al. [10] and $n=111$ of Matsuo et al. [13]) may heavily skew the results towards predominantly emphysematous lobes. Nevertheless, we observed that the average LAA% values of the RUL and the LUL were slightly higher than those of the RLL and the LLL. This is in agreement with the results obtained by Mohamed Hoesein et al. [14]. In particular, we observed that the five-category classification and the PFT measurements showed weak correlations with the LAA% of the RML. This weak correlation had been reported previously by other investigators [10, 13] and may be largely attributed to the relatively small size of the RML. When studying the relationship between the five-category classification and the lobe volumes, as shown in Fig. 6, we found that the volume of the RML did not statistically correlate with the five-category classification ($r=-0.001$, $P=0.976$). This may indicate that the RML inflation is only minimally affected when the severity of emphysema increases. A possible explanation is that the RML is less prone to emphysema. This may be explained by the fact that the average LAA% of RML was smaller than of the other lobes within the range of -920 to -1,000 HU (Fig. 3). In particular, we observed that CT emphysema measurements correlated significantly with the diffusing lung

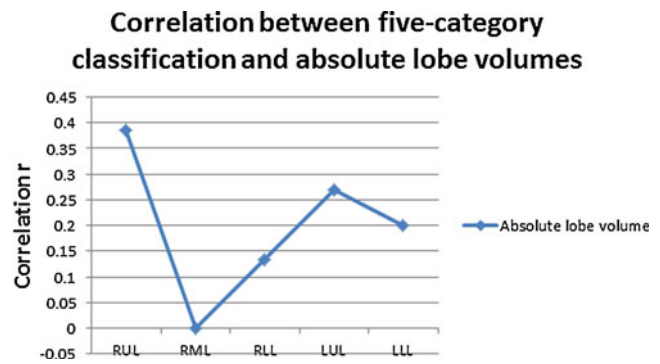
Table 4 Correlations between the percentage of low attenuation area (LAA%) and PFT measurements. The results when the non-COPD subjects were excluded were presented in parentheses

Pulmonary function test measurements						
	RV/TLC (%)	RV (% pred.)	FEV ₁	FEV ₁ (% pred.)	FEV ₁ /FVC (%)	DLeo (%pred.)
RUL	0.563, -945 HU (0.485, -945 HU)	0.632, -930 HU (0.573, -925 HU)	-0.592, -950 HU (-0.546, -945 HU)	-0.683, -940 HU (-0.615, -945 HU)	-0.760, -925 HU (-0.718, -925 HU)	-0.703, -950 HU (-0.696, -950 HU)
RML	0.482, -960 HU (0.416, -965 HU)	0.525, -945 HU (0.460, -950 HU)	-0.511, -965 HU (-0.482, -965 HU)	-0.578, -955 HU (-0.522, -965 HU)	-0.634, -945 HU (-0.585, -950 HU)	-0.528, -965 HU (-0.511, -965 HU)
RLL	0.579, -945 HU (0.524, -945 HU)	0.629, -940 HU (0.579, -935 HU)	-0.582, -945 HU (-0.578, -940 HU)	-0.674, -945 HU (-0.634, -945 HU)	-0.735, -935 HU (-0.718, -935 HU)	-0.625, -950 HU (-0.624, -955 HU)
LUL	0.576, -950 HU (0.518, -950 HU)	0.648, -935 HU (0.607, -930 HU)	-0.578, -960 HU (-0.552, -960 HU)	-0.672, -950 HU (-0.627, -950 HU)	-0.740, -935 HU (-0.715, -935 HU)	-0.651, -955 HU (-0.648, -955 HU)
LLL	0.565, -945 HU (0.511, -945 HU)	0.621, -935 HU (0.574, -935 HU)	-0.544, -945 HU (-0.538, -945 HU)	-0.660, -945 HU (-0.624, -945 HU)	-0.708, -930 HU (-0.685, -930 HU)	-0.563, -950 HU (-0.550, -950 HU)
Upper lobe	0.580, -950 HU (0.513, -950 HU)	0.649, -935 HU (0.600, -930 HU)	-0.599, -960 HU (-0.567, -955 HU)	-0.692, -950 HU (-0.639, -950 HU)	-0.765, -935 HU (-0.735, -930 HU)	-0.688, -955 HU (-0.688, -955 HU)
Lower lobe	0.590, -945 HU (0.539, -945 HU)	0.644, -940 HU (0.599, -935 HU)	-0.582, -945 HU (-0.581, -940 HU)	-0.689, -945 HU (-0.655, -945 HU)	-0.744, -935 HU (-0.729, -935 HU)	-0.619, -950 HU (-0.619, -950 HU)
Left lung	0.606, -950 HU (0.555, -950 HU)	0.675, -935 HU (0.639, -930 HU)	-0.596, -955 HU (-0.586, -950 HU)	-0.708, -945 HU (-0.675, -945 HU)	-0.770, -935 HU (-0.755, -930 HU)	-0.656, -955 HU (-0.660, -955 HU)
Right lung	0.601, -950 HU (0.537, -945 HU)	0.669, -935 HU (0.622, -930 HU)	-0.619, -950 HU (-0.599, -945 HU)	-0.721, -945 HU (-0.673, -945 HU)	-0.794, -930 HU (-0.774, -930 HU)	-0.707, -955 HU (-0.714, -950 HU)
Entire lung	0.613, -950 HU (0.556, -945 HU)	0.681, -935 HU (0.642, -930 HU)	-0.618, -950 HU (-0.605, -945 HU)	-0.726, -945 HU (-0.687, -945 HU)	-0.795, -935 HU (-0.781, -930 HU)	-0.696, -955 HU (-0.706, -955 HU)

All *r* values have *P*<0.001

Table 5 Differences between the highest correlation coefficients and those computed at -950 HU

Lobar configuration	Pulmonary function test measurements					
	RV/TLC (%)	RV (% pred.)	FEV ₁	FEV ₁ (% pred.)	FEV ₁ /FVC (%)	DLco (%pred.)
RUL	0.000 (<i>P</i> =0.5)	0.009 (<i>P</i> =0.401)	0 (<i>P</i> =0.5)	0.002 (<i>P</i> =0.476)	0.015 (<i>P</i> =0.281)	0 (<i>P</i> =0.5)
RML	0.005 (<i>P</i> =0.456)	0.000 (<i>P</i> =0.5)	0.002 (<i>P</i> =0.480)	0.002 (<i>P</i> =0.480)	0.002 (<i>P</i> =0.476)	0.009 (<i>P</i> =0.417)
RLL	0.001 (<i>P</i> =0.488)	0.004 (<i>P</i> =0.456)	0.001 (<i>P</i> =0.488)	0.001 (<i>P</i> =0.488)	0.008 (<i>P</i> =0.386)	0 (<i>P</i> =0.5)
LUL	0 (<i>P</i> =0.5)	0.007 (<i>P</i> =0.421)	0.003 (<i>P</i> =0.468)	0 (<i>P</i> =0.5)	0.010 (<i>P</i> =0.356)	0.001 (<i>P</i> =0.488)
LLL	0.001 (<i>P</i> =0.492)	0.005 (<i>P</i> =0.444)	0.001 (<i>P</i> =0.492)	0.002 (<i>P</i> =0.476)	0.007 (<i>P</i> =0.409)	0.001 (<i>P</i> =0.492)
Upper lobe	0 (<i>P</i> =0.5)	0.006 (<i>P</i> =0.432)	0.002 (<i>P</i> =0.480)	0 (<i>P</i> =0.5)	0.009 (<i>P</i> =0.359)	0.001 (<i>P</i> =0.488)
Lower lobe	0.000 (<i>P</i> =0.5)	0.005 (<i>P</i> =0.444)	0.001 (<i>P</i> =0.488)	0.001 (<i>P</i> =0.488)	0.010 (<i>P</i> =0.356)	0 (<i>P</i> =0.5)
Left lung	0 (<i>P</i> =0.5)	0.005 (<i>P</i> =0.440)	0.000 (<i>P</i> =0.5)	0.000 (<i>P</i> =0.5)	0.010 (<i>P</i> =0.341)	0.001 (<i>P</i> =0.488)
Right lung	0 (<i>P</i> =0.5)	0.006 (<i>P</i> =0.429)	0 (<i>P</i> =0.5)	0.001 (<i>P</i> =0.484)	0.011 (<i>P</i> =0.312)	0.001 (<i>P</i> =0.488)
Whole lung	0 (<i>P</i> =0.5)	0.005 (<i>P</i> =0.436)	0 (<i>P</i> =0.5)	0.001 (<i>P</i> =0.484)	0.010 (<i>P</i> =0.326)	0.001 (<i>P</i> =0.488)

**Fig. 6** Correlations between the five-category classification and lobe volumes. (1) RUL: $r=0.386$, $P<0.001$; (2) RML: -0.001 , $P=0.976$; (3) RLL: 0.135 , $P<0.001$; (4) LUL: 0.269 , $P<0.001$; (5) LLL: $r=0.200$, $P<0.001$

capacity of carbon monoxide (DLco) at levels of both individual lobes and the entire lung. Our results are in consistence with those in [10, 27, 28], suggesting that DLco might be a useful measurement for emphysema diagnosis.

We are aware of the limitations of this study. First, despite the relatively large size of the dataset, the CT examinations in this study are not equally distributed in each category. We note that it is very difficult to have a dataset that can meet such a criterion in practice. Fortunately, our conclusions may not be affected in this study because of the large number of CT examinations in each category. Second, it has been shown that the CT acquisition protocols, such as dose, image reconstruction kernels, and equipment, may have an impact on CT-based quantification [8, 25, 29]. In our study, we did not consider the details in the CT acquisition protocols. For example, the “bone” kernel used in this study may alter the displayed Hounsfield unit number. However, we had shown that the differences in correlation coefficients were very small under the threshold range -925 HU to -965 HU. In addition, Boedeker et al. [30] demonstrated that the “bone” kernel might shift the obtained density mask volume by 2.4 % compared with the “standard” kernel. The underlying implication is that even under different image acquisition protocols we should draw similar conclusions. Nevertheless, this study could be improved by using datasets acquired under different protocols. Third, the CT examinations used in this study were acquired at the end of full inspiration. It is likely that the lung density will vary when chest CT examinations are acquired at the end of full expiration, thereby leading to a completely different optimal threshold for the quantification of emphysema extent. In clinical practice, the CT for emphysema assessment is typically acquired at the end of full inspiration. It may be interesting, however, to investigate the

optimal thresholds for emphysema assessment when CT examinations are acquired at other respiratory stages (e.g. full expiration).

In summary, our study investigated the optimal threshold for computerised tomographic assessment of the extent of emphysema using a large dataset consisting of 573 CT examinations. The density mask method was not only applied to the entire lung but also to each individual lobe. Our results show that the single threshold of -950 HU is optimal for CT densitometry analysis of emphysema when the CT examinations are acquired at full inspiration.

Acknowledgments This work was supported in part by grants HL096613, CA090440, HL084948, HL095397, 2012KTCL03-07 to the University of Pittsburgh from the National Institute of Health, the Bonnie J. Addario Lung Cancer Foundation, and the SPORC in Lung Cancer Career Development Program.

References

- Mao JT, Goldin JG, Dermand J, Ibrahim G, Brown MS, Emerick A, McNitt-Gray MF, Gjertson DW, Estrada F, Tashkin DP, Roth MD (2002) A pilot study of all-trans-retinoic acid for the treatment of human emphysema. *Am J Respir Crit Care Med* 165:718–723
- Müller NL, Staples CA, Miller RR, Abboud RT (1988) “Density mask”. An objective method to quantitate emphysema using computed tomography. *Chest* 94:782–787
- Gevenois PA, de Maertelaer V, De Vuyst P, Zanen J, Yernault JC (1995) Comparison of computed density and macroscopic morphometry in pulmonary emphysema. *Am J Respir Crit Care Med* 152:653–657
- Camicciotoli G, Bartolucci M, Maluccio NM, Moroni C, Mascalchi M, Giuntini C, Pistolesi M (2006) Spirometrically gated high-resolution CT findings in COPD: lung attenuation vs lung function and dyspnea severity. *Chest* 129:558–564
- Marsh S, Aldington S, Williams MV, Nowitz M, Kingzett-Taylor A, Weatherall M, Shirtcliffe P, Pritchard A, Beasley R (2006) Physiological associations of computerized tomography lung density: a factor analysis. *Int J Chron Obstruct Pulmon Dis* 1:181–187
- Madani A, Van Muylem A, Gevenois PA (2010) Pulmonary emphysema: effect of lung volume on objective quantification at thin-section CT. *Radiology* 257:260–268
- Diaz AA, Bartholmai B, San José Estépar R, Ross J, Matsuoka S, Yamashiro T, Hatabu H, Reilly JJ, Silverman EK, Washko GR (2010) Relationship of emphysema and airway disease assessed by CT to exercise capacity in COPD. *Respir Med* 104:1145–1151
- Madani A, De Maertelaer V, Zanen J, Gevenois PA (2007) Pulmonary emphysema: radiation dose and section thickness at multidetector CT quantification—comparison with Macroscopic and Microscopic Morphometry. *Radiology* 243:250–257
- Stavngaard T, Shaker SB, Dirksen A (2006) Quantitative assessment of emphysema distribution in smokers and patients with alpha1-antitrypsin deficiency. *Respir Med* 100:94–100
- Saitoh T, Koba H, Shijubo N, Tanaka H, Sugaya F (2000) Lobar distribution of emphysema in computed tomographic densitometric analysis. *Invest Radiol* 35:235–243
- Revel MP, Faivre JB, Remy-Jardin M, Deken V, Duhamel A, Marquette CH, Tacelli N, Bakai AM, Remy J (2008) Automated lobar quantification of emphysema in patients with severe COPD. *Eur Radiol* 18:2723–2730
- Brown MS, Kim HJ, Abtin FG, Strange C, Galperin-Aizenberg M, Pais R, Da Costa IG, Ordookhani A, Chong D, Ni C, McNitt-Gray MF, Tashkin DP, Goldin JG (2012) Emphysema lung lobe volume reduction: effects on the ipsilateral and contralateral lobes. *Eur Radiol* 22:1547–1555
- Matsuo K, Iwano S, Okada T, Koike W, Naganawa S (2012) 3D-CT Lung volumetry using multidetector row computed tomography: pulmonary function of each anatomic lobe. *J Thorac Imaging* 27:164–170
- Mohamed Hoessein FA, van Rikxoort E, van Ginneken B, de Jong PA, Prokop M, Lammers JW, Zanen P (2012) Computed tomography-quantified emphysema distribution is associated with lung function decline. *Eur Respir J* 40:844–850
- Rabe KF, Hurd S, Anzueto A, Barnes PJ, Buist SA, Calverley P, Fukuchi Y, Jenkins C, Rodriguez-Roisin R, van Weel C, Zielinski J (2007) Global strategy for the diagnosis, management, and prevention of chronic obstructive pulmonary disease: GOLD executive summary. *Am J Respir Crit Care Med* 176:532–555
- Zhang J, Bruesewitz MR, Bartholmai BJ, McCollough CH (2008) Selection of appropriate computed tomographic image reconstruction algorithms for a quantitative multicenter trial of diffuse lung disease. *J Comput Assist Tomogr* 32:233–237
- Pu J, Roos J, Yi CA, Napel S, Rubin GD, Paik DS (2008) Adaptive border marching algorithm: automatic lung segmentation on chest CT images. *Comput Med Imaging Graph* 32:452–462
- Pu J, Leader JK, Zheng B, Knollmann F, Fuhrman C, Sciurba FC, Gur D (2009) A computational geometry approach to automated pulmonary fissure segmentation in CT examinations. *IEEE Trans Med Imaging* 28:710–719
- Pu J, Zheng B, Leader JK, Fuhrman C, Knollmann F, Klym A, Gur D (2009) Pulmonary lobe segmentation in CT examinations using implicit surface fitting. *IEEE Trans Med Imaging* 28:1986–1996
- Nakano Y, Muro S, Sakai H, Hirai T, Chin K, Tsukino M, Nishimura K, Itoh H, Paré PD, Hogg JC, Mishima M (2000) Computed tomographic measurements of airway dimensions and emphysema in smokers. Correlation with lung function. *Am J Respir Crit Care Med* 162:1102–1108
- Park KJ, Bergin CJ, Clausen JL (1999) Quantitation of emphysema with three-dimensional CT densitometry: comparison with two-dimensional analysis, visual emphysema scores, and pulmonary function test results. *Radiology* 211:541–547
- Tanabe N, Muro S, Hirai T, Oguma T, Terada K, Marumo S, Kinose D, Ogawa E, Hoshino Y, Mishima M (2011) Impact of exacerbations on emphysema progression in chronic obstructive pulmonary disease. *Am J Respir Crit Care Med* 183:1653–1659
- Camp PG, Coxson HO, Levy RD, Pillai SG, Anderson W, Vestbo J, Kennedy SM, Silverman EK, Lomas DA, Paré PD (2009) Sex differences in emphysema and airway disease in smokers. *Chest* 136:1480–1488
- Morgan MD (1992) Detection and quantification of pulmonary emphysema by computed tomography: a window of opportunity. *Thorax* 47:1001–1004
- Yuan R, Mayo JR, Hogg JC, Paré PD, McWilliams AM, Lam S, Coxson HO (2007) The effects of radiation dose and CT manufacturer on measurements of lung densitometry. *Chest* 132:617–623
- Pescarolo M, Sverzellati N, Verduri A, Chetta A, Marangio E, De Filippo M, Olivieri D, Zompatori M (2008) How much do GOLD stages reflect CT abnormalities in COPD patients? *Radiol Med* 113:817–829
- Mohamed Hoessein FA, Zanen P, van Ginneken B, van Klaveren RJ, Lammers JW (2011) Association of the transfer coefficient of

- the lung for carbon monoxide with emphysema progression in male smokers. *Eur Respir J* 38:1012–1018
28. Mets OM, Murphy K, Zanen P, Gietema HA, Lammers JW, van Ginneken B, Prokop M, de Jong PA (2012) The relationship between lung function impairment and quantitative computed tomography in chronic obstructive pulmonary disease. *Eur Radiol* 22:120–128
29. Gierada DS, Bierhals AJ, Choong CK, Bartel ST, Ritter JH, Das NA, Hong C, Pilgram TK, Bae KT, Whiting BR, Woods JC, Hogg JC, Lutey BA, Battafarano RJ, Cooper JD, Meyers BF, Patterson GA (2010) Effects of CT section thickness and reconstruction kernel on emphysema quantification relationship to the magnitude of the CT emphysema index. *Acad Radiol* 17:146–156
30. Boedeker KL, McNitt-Gray MF, Rogers SR, Truong DA, Brown MS, Gjertson DW, Goldin JG (2004) Emphysema: effect of reconstruction algorithm on CT imaging measures. *Radiology* 232:295–301